

Design Analysis of Brushless Direct Current Generator

S.R. Shankapal[@], Parikshith Mallya^{@,*}, Jayashree Shivkumar[#], and N. Venkateswaran[#]

[@]Ramaiah University of Applied Sciences, Bengaluru - 560 058, India

[#]Combat Vehicles Research and Development Establishment, Chennai - 600 054, India

*E-mail: parikshith.tce@msruas.ac.in

ABSTRACT

In this work, optimisation of a brushless direct current (BLDC) generator design was undertaken by carrying out an electromagnetic and computational fluid dynamic study. The studies were carried out for different loading-overloading conditions and angular speeds, keeping in consideration the required electrical and thermal parameters, firstly for the initial design and then for optimised designs. In the initial phase, transient electromagnetic simulations were done using Ansys Maxwell to estimate power output, flux densities, heat losses et al. In the next phase, steady state conjugate heat transfer simulations using frozen rotor method for rotating domains were carried out in Ansys CFX using the heat loss values obtained from electromagnetic study in the first phase. The results from conjugate heat transfer were obtained in the form of temperature and flow parameters. After a thorough study and comparison of the results for different designs, obtained in the two phases, it was seen one of the optimised designs showed better electromagnetic, thermal and flow parameters as compared to the initial design and satisfied all the optimum electrical and thermal parameters.

Keywords: BLDC generator; Electromagnetic simulation; Conjugate heat transfer; Frozen rotor method; Computational fluid dynamic

1. INTRODUCTION

5kW brushless direct current (BLDC) generator designed by Combat Vehicles Research and Development Establishment (CVRDE), Chennai consist of two stages namely; main exciter and main generator. The main exciter having field winding in the stator which is controlled by a voltage regulator, a part of generator controller unit (GCU). The main generator has to produce 5kW output power between the speed range of 10500 rpm to 13700 rpm, but it was not giving satisfactory electrical output. Hence it is required to identify the reason for the same and need to arrive at optimal design to satisfy the required electrical output. In order to optimise the DC generator design based on electrical and cooling point of view, CVRDE proposed to conduct coupled electromagnetic, thermal simulation and CFD simulations as per CVRDE specifications at Ramaiah University of Applied Sciences.

2. Electromagnetic analysis

2.1 Cases analysed

Three cases were taken up for this study (as shown in Table 1). For each cases, simulations were conducted separately for the stages of the generator at (as shown in Table 2),

2.2 General Electromagnetic Modelling Procedure

Transient electromagnetic (or Emag) simulations were conducted for the internal stages at various loading conditions

at different angular speeds using Maxwell³. The ambient conditions at which simulations were conducted were hot. The geometry of the generator was provided by CVRDE. The dimensions of the slots, core length, inner and outer core diameter and so forth were measured from the model provided. These values were used to generate the core models in the software. These parameters of the core models were further used to provide a reference for the software against which, the corresponding winding models were subsequently created by the software.

Table 1. Cases for electromagnetic analysis

Notations used	Cases	Notes
IG	Initial geometry	High frequency laminations
OG A	Optimised geometry A	Modified geometry, but with same material
OG B	Optimised geometry B	Essentially OG A, but with windings changed

Table 2. Rotation speeds and loading

S. No.	Case
1.	11000 RPM-Rated load,
2.	11000 RPM-50% Over load,
3.	11000 RPM-100% Over load,
4.	13500 RPM-Rated load
5.	13500 RPM-50% Over load
6.	13500 RPM-100% Over load

2.2.1 Modelling of Core

The material considered for the core, i.e., the stator and rotor are made up of high frequency lamination material. The material properties defined in the software include: B-H curve (or relative permeability), bulk conductivity, B-P curve, mass density, composition (solid or laminated steel), stacking factor (calculated from the lamination thickness), stacking direction.

2.2.2 Modelling of Windings

The material defined for all the windings is copper. The poly-phase windings are Lap type. Using the number of poles and number of slots, the winding diagram was arrived at. Once the windings are modelled to the corresponding cores, the parameters like excitations, number of turns, etc are defined.

2.2.3 Modelling of Magnets in Rotor Stage

The material of the magnets embedded in the rotor is samarium cobalt. The primary field was defined by virtue of the material properties defined for magnets. The orientation of the magnetic fields of the individual magnets were defined by creating local coordinate systems.

2.2.4 Other Settings

There are other setups like defining angular velocity, defining the objects that are supposed to rotate; and master-slave boundaries along with symmetry multiplier settings in the case of symmetric modelling, which were all appropriately setup.

2.3 Modelling of Initial Geometry

2.3.1 Analytical Calculations

(a) Resistances of windings: Resistance of windings were calculated for both cold and hot conditions. The change in the resistivity was calculated for higher temperatures using the relation¹:

$$\rho = \rho_0 [1 + \alpha(T - T_0)]$$

where ρ is the resistivity (Ωm) of the material at the new temperature, ρ_0 is the resistivity (Ωm) of the material at standard temperature, T is the temperature (K) at which resistivity is to be calculated, T_0 is the standard temperature (K) at which ρ_0 is calculated.

Then, the resistances of the windings are calculated using the relation¹:

$$R = \rho * L / A$$

where R is the resistance if the winding (Ω), L is the length of the conductor (m), A is the area of cross section of the wire (mm^2)

(b) Inductances of Windings: The self inductances per phase of all the poly-phase windings are calculated using the relation¹:

$$L = \frac{\mu_0 \pi}{2(p/2)^2} \cdot \frac{T_{ph}^2 \cdot L \cdot r_g}{g_e}$$

where μ_0 is permeability of free space and is equal to $4\pi * 10^{-7}$, p is the number of poles, T_{ph} is the number of turns per phase, L is the core length (mm), r_g is the radius of the core near air gap (mm), g_e is the effective air gap length and is given by the relation:

$$g_e = g * k_g$$

Here g is the real air gap length, k_g is the Carter's coefficient and can be calculated by the relation¹:

$$k_g = \frac{W_t + W_s}{W_t + W_s k_s}$$

Here W_t is the tooth width (mm), W_s is slot width (mm), k_s can be calculated as:

$$k_s = \frac{5g}{5g + W_s}$$

(c) Magneto motive force calculation: To calculate magneto motive force (or mmf), Blondel's two reaction theory is considered. For this, leakage reactance X_L , armature reaction reactance X_{ar} , phase voltage V_{ph} , armature current I , flux per pole, air gap flux density and field current is calculated².

2.3.2 Electromagnetic Simulations

(a) Generator Stage 1: As shown in Fig. 1, a field excitation to develop primary field is given to the winding wound around a bobbin. The bobbin, and the core together are the rotor core components. The DC rotor winding creates the primary magnetic field. The Stator has multiphase lap winding with star connected configuration.

Simulations were conducted for various load conditions for specified speed envelope. In order to simulate the overloaded conditions, the load resistance were recalculated to reflect additional load, and the field excitation was increased to compensate for the reduction in terminal voltage, in order to get desired voltage.

Also, it can be seen from the open circuit characteristics that the output curve is saturating at about 3.5A of field current (As shown in Fig. 2).

(b) Stage 2: In the generator stage 2 (As shown in Fig. 3), the primary field is setup by means of a DC current to the stator windings. The field current is defined based on the condition at which simulation is run. The rotor has three phase lap winding connected through star configuration. The rectified output from stage generator 2 is used to setup the primary field in the rotor of stage 1.

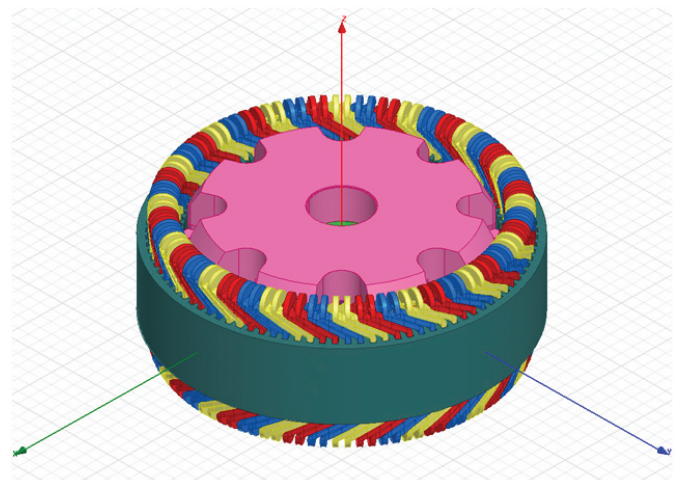


Figure 1. Generator stage 1.

- (c) Losses: Core and copper loss values³ at various simulation conditions are tabulated follows, as shown in Tables 3 and 4).

2.4 Benchmarking and Modelling of Other Cases

Analytical hand calculations were done for a case of the initial geometry and an optimised geometry. Simulations were conducted at those conditions. The analytically calculated values were found to be in agreement to the results obtained by simulation As shown in Table 5. Based on this, the Emag simulation setup methodology was applied to all other cases and simulations were run³.

Similarly, for OG A, as was done for initial geometry, resistance, inductances of windings and the loss values of all the stages were calculated. For OG B as well, resistance, inductances of windings and the loss values of all the the stages were calculated similarly.

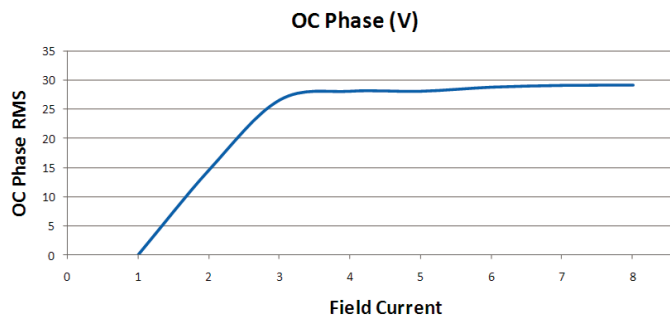


Figure 2. Open circuit characteristics.

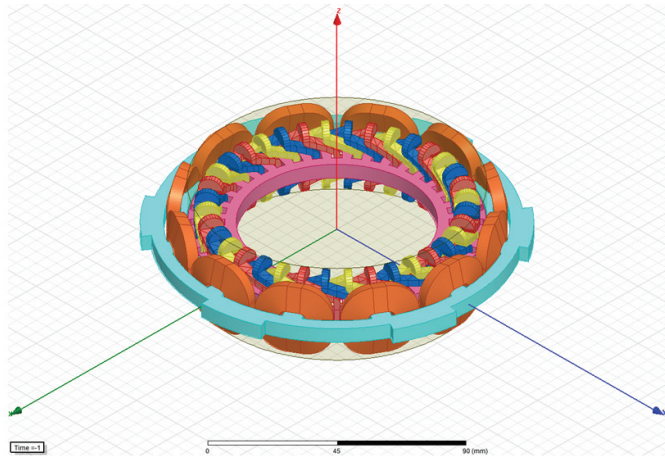


Figure 3. Main exciter stage.

Table 3. Copper and core losses (11000 rpm)

		11000 rpm			
		Rated loaded		50% Over loaded	
		Copper loss	Core loss	Copper loss	Core loss
Stage-1	Stator	3.8	-	10.11465	
	Rotor	7.23	24.72	19.79705	41.61
Stage-2	Rotor	32.14	-	91.9087	
	Stator	435.87	430.11	901.8341	445.83
Output power		5221.65		7383.41	

Table 4. Copper and core losses (13500 rpm)

		13500 rpm			
		Rated loaded		50 % over loaded	
		Copper loss	Core loss	Copper loss	Core loss
Stage-1	Stator	2.25		5.67	
	Rotor	5.25	28.45	14.60	52.01
Stage-2	Rotor	21.16		53.25	
	Stator	351.16	508.34	700.12	715.44
Output power		5194.16		7736.83	

3. THERMAL ANALYSIS

3.1 Cases Analysed

Two geometries were considered, an initial geometry and then an optimised geometry B. Two different speeds of 11000rpm, 13500 rpm were considered and three loading conditions of rated, 50 per cent over load and 100 per cent over load. Initially 10 cases were analysed and CFD simulations were done for them as shown in Table 6 and Table 7).

Table 5. Comparison between hand calculation and simulation values

		Calculated	Simulated
Input field current	I_f	0.81 A	0.81 A
Rectified DC current	I_{DC}	3.30 A	3.23 A
Rectified DC voltage	V_{DC}	8.74 V	8.56 V
Indtance per phase	L_{ph}	293.69 μ H	341.2 μ H
Phase current, RMS	I_{ph}	2.69 A	2.70 A
Phase voltage, RMS	V_{ph}	3.73 V	4.80 V
		Calculated	Simulated
Input field current	I_f	2.77 A	2.66 A
Rectified DC current	I_{DC}	3.33 A	3.35 A
Rectified DC voltage	V_{DC}	20.60 V	20.71 V
Indtance per phase	L_{ph}	511.16 μ H	448.26 μ H
Phase current, RMS	I_{ph}	2.72 A	3.01 A

3.2 General Thermal Modelling Procedure

The general procedure that has been followed for the conjugate heat transfer simulation is as follows:

- The flow domain is extracted from the given geometry using a CAD software
- Using HYPERMESH pre-processor tool, the flow domain as well as the solid region is discretised for the conjugate heat transfer analysis
- Applying the appropriate boundary conditions, the flow domain is prepared for the solver ANSYS CFX (loss values from EMAG simulation are taken and wattage is calculated) and a steady state simulation is executed⁴
- The solution was iterated upon till convergence of all the transport variables.

3.3 Computational Model

The computational domain was discretised with about

Table 6. Initial geometry

S. No.	Case
1.	11000RPM-Rated load
2.	11000RPM-50 per cent over load
3.	13500RPM-Rated load
4.	13500RPM-50 per cent over load

Table 7. Optimised geometry

S. No.	Case
1.	11000RPM-Rated load
2.	11000RPM-50 per cent over load
3.	11000RPM-100 per cent over load
4.	13500RPM-Rated load
5.	13500RPM-50 per cent over load
6.	13500RPM-100 per cent over load

3674199 (i.e. 2061154 fluid and 1613045 solid elements) unstructured tetrahedral cells for computational model of initial geometry and 2627167 (i.e. 1426776 fluid and 1200391 solid elements) unstructured tetrahedral cells for computational model of OG B. The computational model was divided into three distinct regions: stationary fluid meshed region, rotating fluid meshed region and solid meshed region as shown below. The mesh was also suitably modified for all trials of OG B that required modification of components. Figure 4 shows the fully meshed model of IG. Figure 5 shows the mesh for different regions of OG.

3.4 Boundary Conditions

Pressure inlet and pressure outlet boundary condition is taken for the inlet and outlets. Reference pressure is taken as one atmosphere (except for altitude case). Frozen rotor approach was used for rotating regions⁴. The K-Epsilon turbulence model was employed to model the turbulent flow equations. Interfaces were created between different components. The losses from Emag simulations and frictional losses were used as heat sources. Tables 8 and 9 shows the heat source value.

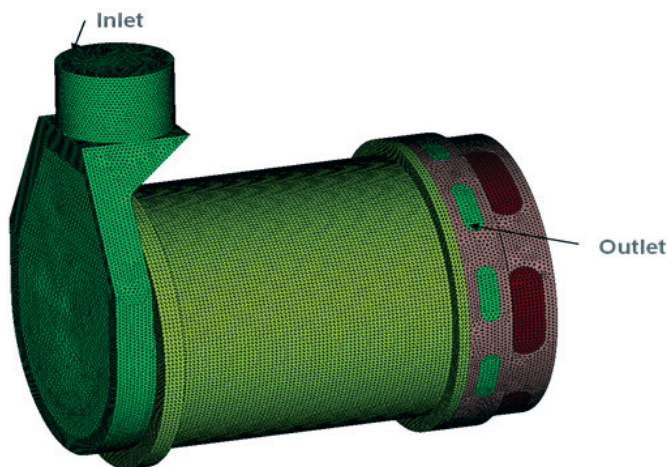


Figure 4. Fully meshed model of initial geometry.



Figure 5. Optimised geometry (stationary fluid mesh, rotating fluid mesh, solid mesh - Stator rotor windings and core mesh and yoke).

Table 8. Wattage for initial geometry - 11000 rpm and rated loading

Part	Watt (from Emag)	Source (W/m ³)
Stage1_Rotor_Core	24.71	1300415
Stage2_Stator_Core	430.11	4469080
Stage1_Stator_Winding	3.79	118391.5
Stage1_Rotor_Winding	7.23	258089.1
Stage1_Rotorrobin	32.14	307286.9
Stage2_Stator_Winding_	435.87	4466414
heat loss	933.8	

Total power generated (from EMAG) - 5221.65 Watts

Table 9. Friction-mechanical losses for initial geometry - 11000 rpm and rated loading

Part	Watt (from Emag)	Source (W/m ³)
Shaft	261.08	5993742.72
De bearing	130.54	5369098.77
Yoke bearing	130.54	7188551.18
Heat loss	522.17	

Extra 10 per cent of total power generated (i.e 522.165 W) load applied on De bearing, Yoke bearing and shaft (friction and mechanical losses).

4. RESULTS AND DISCUSSION

As seen above, numerous simulations were done for both Electromagnetic and thermal studies. Results in the form of plots for flux density, thermal contours, flow path lines etc were obtained from these simulations. Figures 6 and 7 show the flux density plot obtained for different stages from Emag simulation. Figures 8 and 9 show the plots from CFD for initial geometry at rated loading. Figures 10 and 11 show the OG B domain model and flow pathlines in it for that case obtained from CFD.

The observations that can be made from these studies are as follows:

4.1 Electromagnetic Studies

The electromagnetic simulations were conducted for the optimised geometry. The results indicated that the optimised Generator Stage-1 was satisfactorily meeting the output power

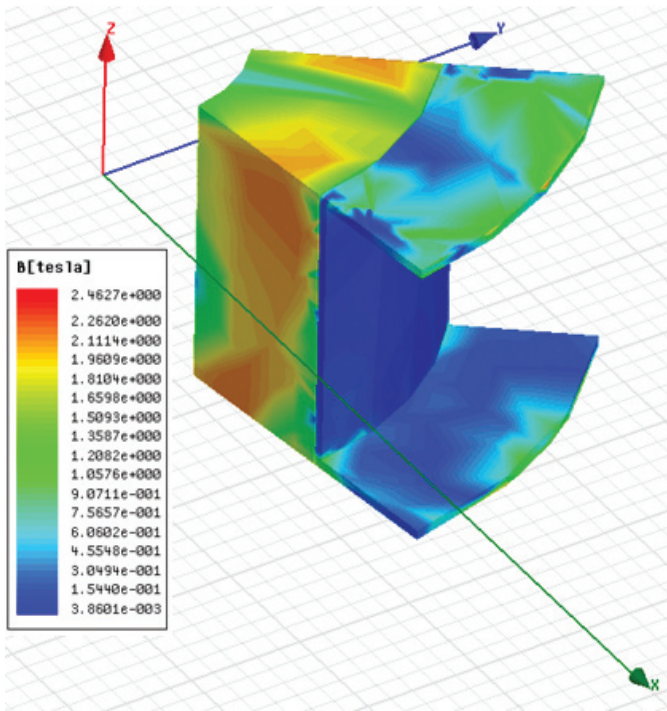


Figure 6. Flux density plot of stage1 stator.

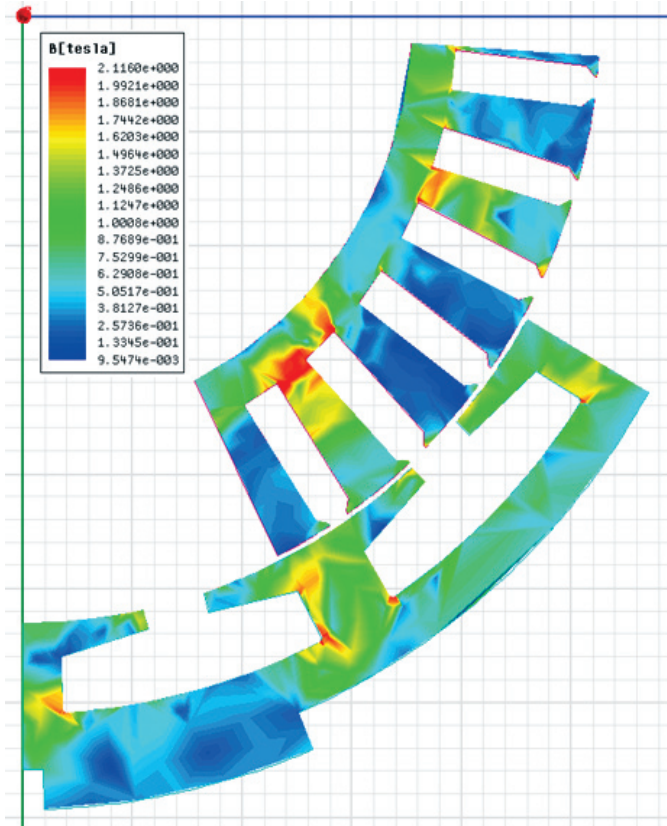


Figure 7. Flux density plot of stage 2 stator and rotor.

requirement (loaded and overload) condition. Furthermore, the rectified output from the rotor of the stage-2 was found to be sufficient enough to set up the primary field in the rotor of the generator stage 1.

The electromagnetic simulations for the optimised

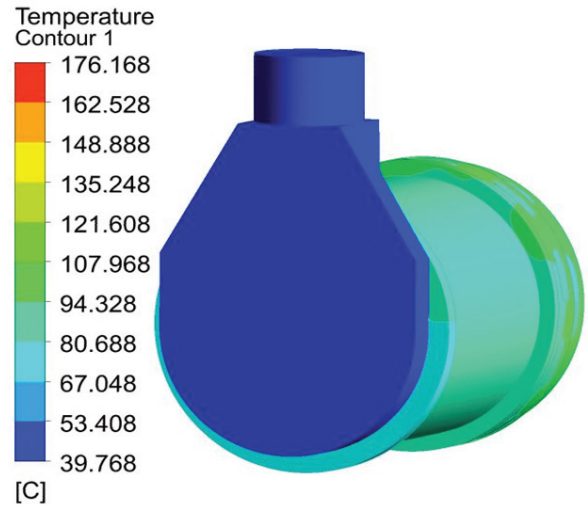


Figure 8. Thermal contour on entire domain (IG).

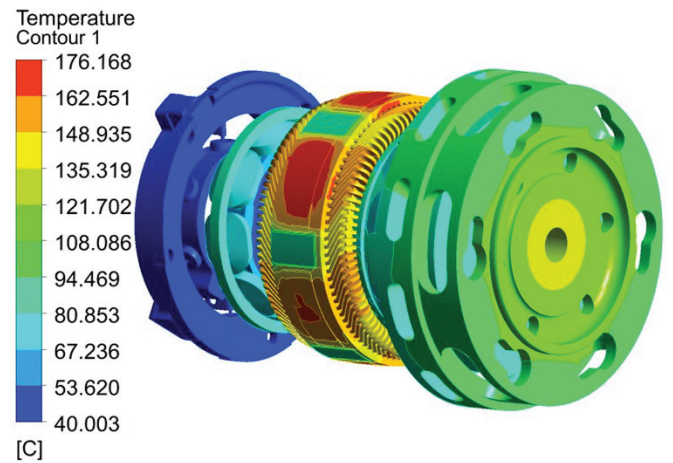


Figure 9. Thermal contour on entire domain (IG).

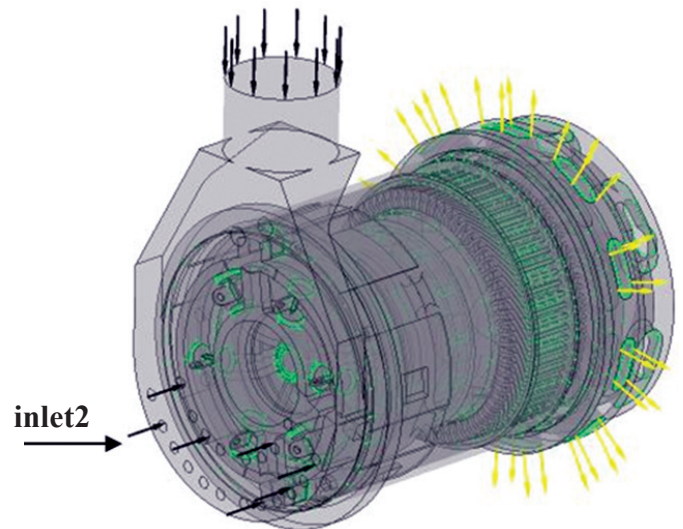


Figure 10. OG B domain with inlet2.

geometry with changed winding parameters were also conducted. Just like in the case explained in the preceding paragraph, output at loaded and overload conditions were satisfactorily obtained.

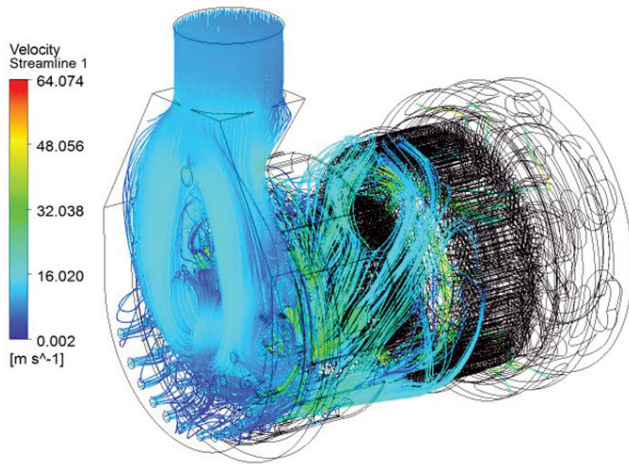


Figure 11. Flow pathlines for OG B with inlet2.

The hand calculations of various parameters like inductance, losses, phase current, flux per pole, rectified output and so forth were matching the values obtained in the simulations. The loss values obtained at various components like windings and cores were subsequently provided to the CFD team for further thermal analysis of the generator assembly.

4.2 Thermal Studies

For the initial geometry, it is seen that maximum temperature region is seen in the stage-1 stator core region for all the loading cases, while for OG B it is seen in stage-1 stator winding. While, for both IG and OG B, as rotation speed increases, mass flow rate and flow velocity increased. OG B gave better performance parameters in terms of higher mass flow rate, less temperature readings as compared to IG

For OG B with inlet2 (OG B with small holes in the form of secondary inlets), the temperatures were just a bit lower than OG B.

5. CONCLUSIONS

An extensive electromagnetic and thermal study were undertaken on a given initial geometry of BLDC generator and then modified geometries of the BLDC generator for different loading conditions etc. This study was helpful in understanding the electrical and thermal performance for these cases, in providing an insight into the flow, velocity and thermal profile inside the generator for these cases. All the information gained from this study has proved helpful in helping us come up with a better design of the BLDC generator which is a substantial improvement from the initial geometry design.

REFERENCES

1. Sawhney, A.K. A Course in electrical machine design. Ed. 6. Dhanpat Rai and Sons, 2006.
2. Phil Corso, P.E. The physics of armature-reaction. Boca Raton, Florida, 05-Jan-2007.
3. Ansys Maxwell help manual.
4. Ansys CFX help manual.

CONTRIBUTORS

Dr S.R. Shankapal was working as Vice Chancellor of M.S. Ramaiah University of Applied Sciences since January 2014. He earned his PhD degree from BITS-Pilani, in the area of thermodynamic and Energy conversion, he has been teaching for the last 30 years. He has conducted hundreds of training programmes for practicing engineers of leading automotive and engineering companies all over India. He has guided more than 100 UG, PG students and a few PhD Scholars. He has been awarded research grants exceeding Rs. 5 crores. He coordinated an international project that was awarded under EU-FP6 as well as UKIERI Project awarded by the British Council UK. He has published more than 75 research papers in journals and conferences and delivered more than 75 lectures during seminars and symposia held in India and abroad and written 9 books. He has 3 patents to his credit.

Mr Parikshith Mallya is working as Technical Manager of Techno centre engineering, Ramaiah University of Applied Sciences since August 2010. He earned his Master degree from Ramaiah University, in the area of automotive engineering. He has involved in the design and development of automotive torque converter code and many mechanical system design related project. He is having more than 8 years of experience in Thermal Design/Analysis, Computational Fluid Dynamics and Fluid Structure Interaction related simulations and he has executed many projects for public sectors, MSME and Defence organizations (DRDO).

Ms Jayashree Shivkumar, has completed BE in Electrical and Electronic Engineering from GCT, Coimbatore in 1984. Currently she is working as a Scientist 'G', at CVRDE, Chennai. Over seen the installation of Electrical Sub System in 'Main Battle Tank, Arjun', prototype. Responsible for Design and Development of automatic gear controller for indigenous transmission for power pack. Later completed MTech in Controls Guidance And Instrumentation in 1992 From IIT Chennai. Project coordinator for instrumentation and testing of Aircraft Accessories for Tejas, LCA. Project leader for the Design, Development and Testing of multistage PM generators and Electric drives. She has published more than 8 papers in National/International conferences.

Mr N. Venkateswaran, has obtained his AMIE (Mech. Engg.) from the Institute of Engineers, Kolkata, in 1988. In 1995, He completed his ME (Thermal power) from the Annamalai University. Currently he is working as a Scientist 'E' at CVRDE, Chennai. He has worked on the development of cooling system and heat exchangers in the armoured tracked vehicles. For the past fifteen years, he is working at the Centre for Engineering Analysis and Design (CEAD), where he is engaged in various FE-based analysis software's and carried out the estimation of critical speed of driving system of armoured fighting vehicles. He has also carried out Heat transfer and thermo mechanical analysis of various IC engine sub systems. He has imparted more contributions on torsional vibration study of entire crank train of Armoured fighting vehicles Engines.